Hybrid Navigation System for Long Range Operation

M. João Rendas Isabel M. G. Lourtie

ISR/ Instituto Superior Técnico, Depart. Eng. Electr. & Comp.
Av.Rovisco Pais, P-1096 Lisboa Codex Portugal

Abstract In this paper we describe a navigation system that allows long range navigation by combining two distinct modes: local positioning with respect to a long baseline array of known localization (reference points) and autonomous mode in-between reference points, relying only on sonar/Doppler and depth information. The areas of transponder-based navigation are defined by the maximum range of transponder operation. In both modes, a Kalman based design approach was chosen, using, when necessary, the available position estimates to characterize the errors associated with the filter inputs. We present simulation results that illustrate system's behavior for a typical maneuvering operation.

I. Introduction

To achieve a truly autonomous behavior, an autonomous underwater vehicle (AUV) must be able to locate itself in the operating scenario. The navigation system, an essential module in any AUV, is the responsible to provide, at any time instant, an estimate of its position and velocity with respect to a prescribed referential. This information must be available so that control of its motion and path planning can be defined according to the task to be performed.

Several configurations may be possible, depending on the application and the propagation characteristics of the environment. For instance, in highly structured ambients, navigation can be based on a pre-existing map, with online recognition of relevant features of that map on the surrounding scene. In unstructured scenarios, like for underwater robotics, no such map exists in general, and navigation must resort to odometry and/or the presence of recognizable landmarks of known position. In most situations, each form of navigation is not sufficient by itself: systems based only on local features or landmarks can exhibit satisfactory behavior only on restricted areas, while systems based on odometry data alone tend to present a degrading performance, resulting, for missions of a reasonable extent, in an unacceptable error level.

The system described in this paper allows extendedrange navigation by combining two distinct modes: local positioning with respect to a long baseline array of known localization (reference points) and autonomous mode in-between reference points, relying only on sonar/Doppler and depth information, see Figure 1.

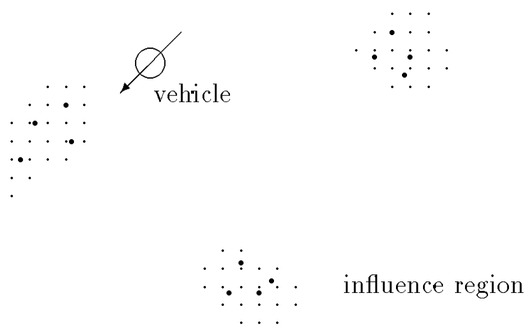

Figure 1: Long Range Operation.

In this way, the vehicle is able to navigate in large areas, acquiring precise knowledge of its position by locking into one of the dispersed reference points, and admitting an increasing error during its autonomous phase. With this architecture, the position of the baseline arrays and the design of the vehicle's mission must be compatible with each other, i.e., the uncertainty margin must be limited by imposing a maximum duration to each period of autonomous navigation.

The areas of transponder based navigation are defined by the maximum operating range associated to each transpoder. As the system is leaving the area where a particular baseline array is located, the number of range measurements it is able to receive will gradually decrease to zero, entering, in this way, the autonomous navigation mode. On the contrary, when it approaches an area where transponders are located, it receives an increasing number of distance measurements, switching from autonomous to local navigation mode.

Figure 2 shows a functional block of the hybrid navigation system. The two main blocks correspond to each possible mode of operation: local and autonomous. The interrogation block uses the estimated vehicle position and the error prediction to determine its proximity to one of

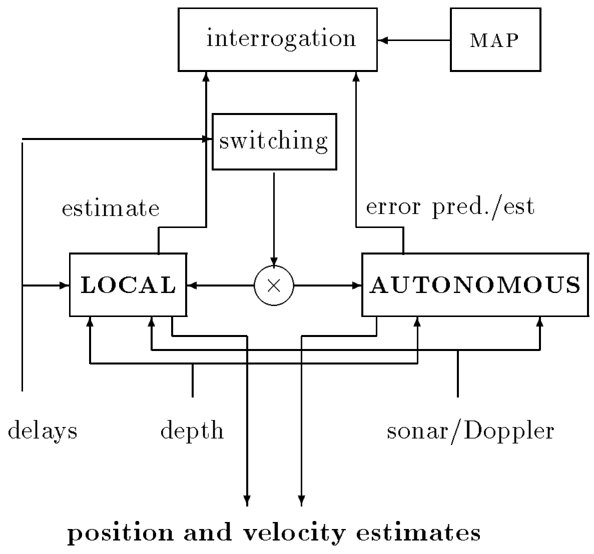

Figure 2: Block diagram of the navigation system.

the baseline arrays, deciding on the need to send an interrogation signal. The baseline arrays are distinguished by the answering frequencies of their transponders.

A switching module determines, based on the number of transponder answers, the convenient navigation mode (local or automous).

For both modules, a Kalman filtering model based design approach has been used, with appropriate modeling of the statistical charaterization of the filter's inputs [1]. Since most of the time the expected vehicle's acceleration is close to zero, becoming non-zero only during maneuvering situations, we implemented a variable dimension Kalman filter [2]. With this filter, when the vehicle's movement is uniform, the Kalman filter assumes the acceleration is zero and estimates just the position and the linear velocity (quiescent model). Each time a maneuver is detected, the Kalman filter switches to a larger order (maneuvering model) extending its state vector to include the vehicle's accelerations.

The paper is organized in the following way. In section **II** we briefly describe the transponder based navigation mode. Section **III** is devoted to the autonomous mode. Simulation results of the hybrid navigation system are presented for a typical maneuvering situation in section **IV**. Finally, section **V** concludes the paper, presenting some ideas for future work.

II. Transponder Based Navigation

The local navigation mode assumes, in addition to odometry data (depth and sonar/Doppler measurements), the existence of an hydrophone/projector unit located on the vehicle, and of an array of four subsea transponders located near the sea bottom, at ranges that allow transponder interrogation by the vehicle. The hydrophone/projector unit on the AUV interrogates the four subsea transponders. These transmit an acoustic pulse when the vehicle's interrogation pulse is received. The operating frequency and power of transmitted signals imposes a maximum distance between the vehicle and the transponders, beyond which no operation is possible. The two-way range between the vehicle and each transponder unit is computed based on the round-trip transmission time.

The problem geometry is depicted in Figure 3 [3], and a block diagram of the navigation system in Figure 4.

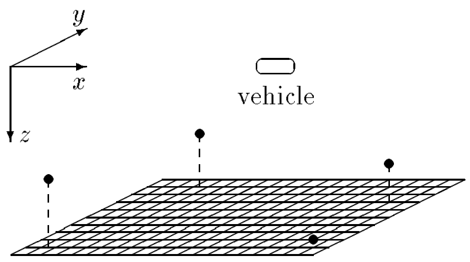

Figure 3: Problem geometry.

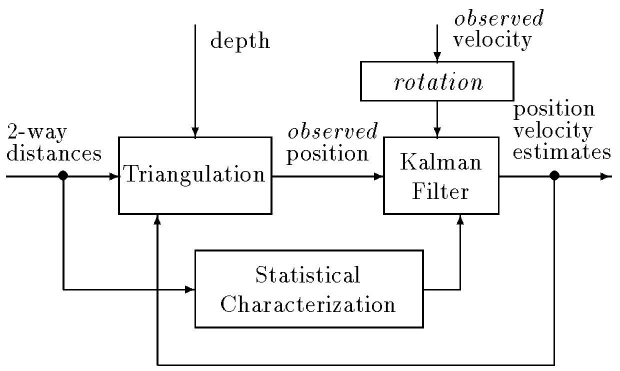

Figure 4: Local Navigation System.

We identify two main blocks in Figure 4: the *triangulation block*, that performs the geometric transformation between the measured ranges and the vehicle's position, and the *Kalman filtering block* that carries out a temporal filtering of the observed series.

This structure corresponds to a simplification of the optimal non-linear estimator for this problem, dealing with the non-linearity of the observations within the triangulation block, and solving afterwards a linear filtering problem. To minimize the effects of this decoupling, one must assure that an accurate statistical characterization of the observations at the filter input is available, at each time instant.

The four transponder units T_i, $i = 1, 2, 3, 4$, are located at positions (x_i, y_i, z_i). The inertial frame is defined with respect to the transponder positions, as shown in Figure 3. In the sequel, we assume that the transponder locations are *a priori* known. Ranges R_i $(i = 1, \ldots, 4)$ from the subsea unit i to the vehicle's position (r_x, r_y, r_z) on the k^{th} interrogation, computed as half of the two-way measured ranges, are given by

$$R_i^2 = (r_x - x_i)^2 + (r_y - y_i)^2 + (r_z - z_i)^2 \quad . \tag{1}$$

For error free range measurements, the vehicle's location is given by the intersection point of four spheres with radius R_i, which are centered at each transponder unit i, respectively.

Since range is measured with error, situations may arise where, for the set of available measurements, a solution does not exist. Denoting by Dist_{ij} the distance between transponders i and j, a necessary condition for the existence of a solution is that

$$\begin{array}{rcl} R_i + R_j & > & \text{Dist}_{ij} \\ |R_i - R_j| & < & \text{Dist}_{ij} \end{array} \quad , \; i \neq j \quad , \tag{2}$$

are both satisfied by each pair of transponders. In other words, the two spheres centered on each pair of transponders have a non-empty intersection. Whenever a solution cannot be found with the available set of range measurements, we validate those measurements that are closer to the ranges predicted by the Kalman filter position estimate.

The triangulation routine takes into account the possibility of misfunction (no measurement) of one or more transponder units, and/or the presence of outliers in the range measurements, that is, it computes a *measurement* of the vehicle's position provided that at least one range measurement is available. This is particularly important when the vehicle is either leaving or approaching an area covered by one of the baseline arrays.

When four, or three range measurements are available, r_x and r_y can be linearly related to r_z based on the differences $R_i^2 - R_j^2$ taken for $i \neq j$. Since the depth, r_z, is measured independently, no ambiguity arises when computing the vehicle's position by triangulation techniques. On the contrary, although two range and depth measurements is still enough to compute the vehicle's position, ambiguity results from the non-linear character of the relationship between range and position. This ambiguity is removed by choosing the solution closest to the Kalman filter predicted estimates $(\hat{x}, \hat{y}, \hat{z})$. Finally, when just one range and depth measurements are available, we take for the vehicle's observed position the point of the ambiguity curve that lies closer to the propagated trajectory. This is achieved by minimizing the functional

$$J = (r_x - \hat{x})^2 + (r_y - \hat{y})^2 + (r_z - \hat{z})^2 \tag{3}$$

under the constraints resulting from the available range and depth measurements.

The round–trip travel time measurement errors propagate through the triangulation routine, giving rise to errors in the computation of the vehicle's linear position (r_x, r_y, r_z). These errors, which represent the observation noise of the position data at the input of the Kalman filter, are highly non-homogeneous, the larger uncertainties being obtained for locations either near the sea bottom, or outside the convex region delimited by the subsea transponder units. Different patterns are achieved depending on the number of transponders and their relative location.

The statistical characterization of the position measurement vector is performed on-line, being accomplished by taking a first order approximation of the expressions resulting from the triangulation procedure [1]. The covariance matrix is computed assuming that *(i)* the Kalman filter position estimate is a zero mean Gaussian vector process, and *(ii)* the range measurements R_i are mutually independent uniformly distributed random variables.

The velocity measurements provided by the sonar/Doppler system are reported to the vehicle's coordinate system. Since the navigation system operates in a global inertial frame, a rotation transformation must be applied, depending on the values of the roll, pitch and yaw angles, that relate the two coordinate systems. This transformation is performed by the block *rotation* in Figure 2. In this paper, we assume that the roll, pitch and yaw angles are accurately known.

The estimation of the vehicle's position and linear velocity is carried out by a Kalman filter. Since most of the time the expected vehicle's acceleration is close to zero, becoming non-zero only during maneuvering situations, we implemented a variable dimension Kalman filter [2] in the navigation system. With this filter, when the vehicle's movement is uniform, the Kalman filter assumes the acceleration is zero and estimates just the position and the linear velocity (quiescent model). Each time a maneuver is detected, the Kalman filter switchs to a larger order model (maneuvering model) extending its state vector to include the vehicle's accelerations.

To decide whether the vehicle is maneuvering or not, and which model must be used, a test is performed. When the quiescent model is in use, i.e., the vehicle is not maneuvering, the hypothesis that a maneuver is taking place is accepted if a test variable based on the filter innovations is larger than a given threshold. The threshold adopted in the filter is such that the probability of false alarm in detecting a maneuver is around 5%.

To switch from the maneuvering back to the quiescent model, the estimated accelerations are compared to their standard deviations. If they are not statistically significant the maneuver hypothesis is rejected.

This algorithm is presented and discussed in [2].

The (non-stationary and non-periodic) Kalman filter used in this mode has the following state-space/observations model:

$$\begin{aligned}\sigma(t_k) &= \mathbf{A}(t_k, t_{k-1})\sigma(t_{k-1}) + \mathbf{B}u(t_{k-1}) \\ z(t_k) &= \mathbf{C}\sigma(t_k) + \mathbf{D}v(t_k)\end{aligned}$$

where $\sigma(t_k)$ is the state vector, that can have dimension 6 or 9 (for quiescent and maneuvering models, respectively), $u(t_k)$ is a white sequence modeling velocity (quiescent) or acceleration (maneuvering) variations, and $v(t_k)$ models the non-stationary observation noise (measurements errors). The observations $z(t_k)$ are, for the local navigation system, a 6 dimensional vector, gathering the position estimates produced by the triangulation routine, and the odometry data provided by the sonar/Doppler system.

The vehicle's motion model is obtained based on the law that describes the movement of a point in space, that is, defining the quiscent model state vector as $\sigma = [x\ v_x\ y\ v_y\ z\ v_z]^T$, and denoting by A_6 the system matrix for this case, we have

$$A_6 = \begin{bmatrix} \mathcal{A} & 0 & 0 \\ 0 & \mathcal{A} & 0 \\ 0 & 0 & \mathcal{A} \end{bmatrix} \quad ,$$

where

$$\mathcal{A} = \begin{bmatrix} 1 & t_k - t_{k-1} \\ 0 & 1 \end{bmatrix}$$

is a 2×2 matrix that characterizes the vehicle's dynamic along each coordinate. The input matrix B_6 is, in this case, given by

$$B_6 = \begin{bmatrix} \mathcal{B} & 0 & 0 \\ 0 & \mathcal{B} & 0 \\ 0 & 0 & \mathcal{B} \end{bmatrix} \quad ,$$

where

$$\mathcal{B} = \begin{bmatrix} (t_k - t_{k-1})^2/2 \\ t_k - t_{k-1} \end{bmatrix}$$

is a 2-dimensional vector, while the output matrix C_6 is

$$C_6 = I_6 \quad .$$

When the maneuvering model is being used, the last three components of the state vector are the accelerations (a_x, a_y, a_z) along each coordinate. In this case, the matrices describing the state-space model, A_9 and B_9, are

$$A_9 = \begin{bmatrix} A_6 & B_6 \\ 0 & I_3 \end{bmatrix} \quad ,$$

where I_3 stands for the 3×3 identity matrix, and

$$B_9 = \begin{bmatrix} \mathcal{B} & 0 & 0 \\ 0 & \mathcal{B} & 0 \\ 0 & 0 & \mathcal{B} \\ (t_k - t_{k-1}) & 0 & 0 \\ 0 & (t_k - t_{k-1}) & 0 \\ 0 & 0 & (t_k - t_{k-1}) \end{bmatrix}$$

where $\mathcal{B}$ has been redefined as

$$\mathcal{B} = \begin{bmatrix} (t_k - t_{k-1})^3/6 \\ (t_k - t_{k-1})^2/2 \end{bmatrix} \quad .$$

Regarding the output matrix C_9, we have

$$C_9 = [C_6\ \ 0] \quad .$$

III. Autonomous Navigation

The autonoumos navigation system is based on the availability of a reduced set of measurements when compared to the previous section. Since no transponder based measurements are available in this situation, the navigation system consits only of a Kalman filter that propagates the vehicle's dynamics according to the measured values of linear velocity along each coordinate, and to the output of the depth sensor. A block diagram is shown in Figure 5.

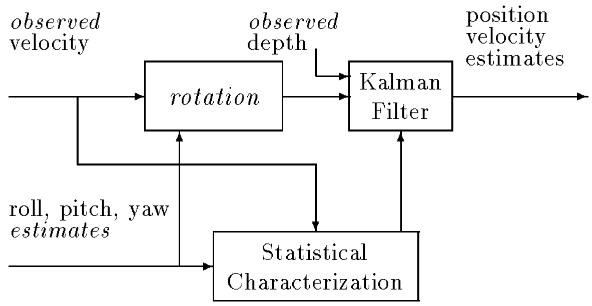

Figure 5: Autonomous navigation system.

The filter structure is the same has in the previous section, with a convenient re-interpretation of the observation vector $z(t_k)$, which is now of dimension 4, one for depth, and the other 3 for velocity. Since we are assuming the rotation transformation relating the vehicle and the inertial frames is accurately known, the input noise to the Kalman filter is, in this case, stationary, and thus there is no need to compute, at each step, the covariance matrix associated to the measurement errors. Due to the non-linear dependence of the transformation matrix on the roll, pitch and yaw angles, this is not the case when taking into account the error in measuring these angles. In this case, an approach similar to the one taken to characterize the transponder based position measurement error in the triangulation routine could be considered. Moreover, since this Kalman filter does not rely on time delay measurements, it works with periodic observations.

To reduce battery comsuption, it is possible, in this mode, to inhibit transponder interrogation when the estimated position falls outside the influence region of the available baseline arrays. This is done by the interrogation system in Figure 2. When autonomous navigation mode is entered, transponder interrogation is inhibited, and position estimates are periodically produced on the basis of the on-board measurement systems (depth sensors and sonar/Doppler). Each time the position estimate is updated, the vehicle determines its proximity to one of the baseline arrays using the current position estimate and its error characterization (provided by the Kalman filter). Based on this determination, transponder interrogation may be re-initialized.

IV. SIMULATIONS

In this section we present simulations of the hybrid navigation system described for a typical vehicle trajectory. In the simulated scenario, two base-line arrays are available. The vehicle starts its trajectory near one of the arrays, and navigates towards the second array in stationary motion, simulating, in this way, navigation between two regions where some taks is to be performed, and where precise information on its position may be required.

Each base-line array of (four) transponder units defines a square in the horizontal ((x, y)) plane with 70 m sides. All transponder units are located in the sea bottom, at a depth of 100 m. The round-trip range masurement errors are modeled as a symmetric uniform random variable in the interval $[-1, 1]$ m. The maximum range for transponder operation is 300 m, and the two base-line arrays are centered around positions $(35, 35)$ and $(1515, 715)$, as shown in Figure 6 (black squares).

The AUV's trajectory starts at instant 0 at the point $(0, 0)$ in the horizontal plane, near the array located near the origin of the coordinate system, and is completely contained in the horizontal plane corresponding to $depth = 60m$. From that point, the vehicle travels towards the other group of transponders, completing its motion at $T = 600$. In the regions near the base-line arrays the vehicle's motion is uniformly accelerated (positive acceleration of $.04ms^{-2}$ in the x direction, and $.02ms^{-2}$ along y in the first – $t < T/8$ –segment, and symmetric values near the distant array – $7/8T < t < T$), while in-between transponder groups, a uniform motion is imposed. The temporal evolution of the vehicle in the (x, y) plane is also shown in Figure 6, the vertical axis denoting time (in seconds).

A first 50 run Monte Carlo experiment was conducted with base-line arrays located closer to each other than in Figure 6, the achieved position mean squared error along each coordinate being shown in Figure 7, while the error evolution along one Monte Carlo run is displayed in Figure 8. For this simulation, the period of uniform motion is $t \in [T/4, 3T/4]$, and the errors in velocity measurements along each 3D coordinate were modelled as random variables uniformly distributed in the interval $[-0.3, 0.3]$ m/s.

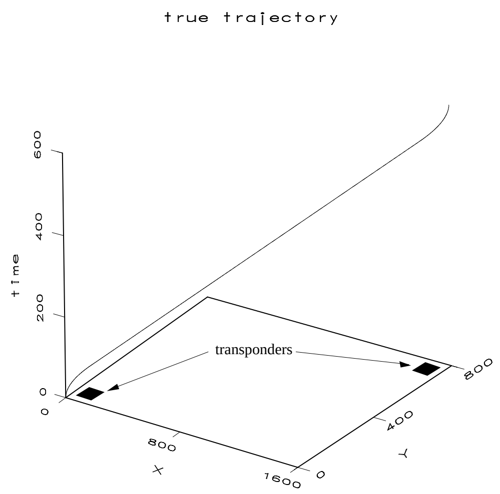

Figure 6: vehicle trajectory and base-line arrays localization.

The error in the depth measurements are uniform, with a maximum absolute value of 0.5 m.

In both figures, the larger errors are observed along the x coordinate, this fact being a consequence of the larger velocity in this direction. The smaller errors are observed along the z coordinate, whixh is explained by the good observability conditions relative to both arrays (much lower depth than transponders), and by the additional depth measurement provided by the dedicated sensor. Analysis of these figures show the expected behavior, with small error values near the base-line arrays, and increasing error during autonomous navigation.

The increasing error behaviour becomes more evident in Figure 9 that shows the error evolution along one Monte Carlo run for widely separated base-line arrays (second set of transponders located around $(1515, 715)$ as in Figure 6). In this case, the ime interval of analysis has been increased to $T = 600$ seconds, and the interval of uniform motion is $t \in [T/8, 7T/8]$.

Figures 10 and 11 illustrate the error behavior under reduced velocity measurement errors. The two sets of transponders are located as in Figure 9 and the vehicle trajectory is also the same, but in this case the error in the velocity measurements is smaller, having a uniform distribution with a maximum absolute value of 0.1 m/s.

Comparison of Figures 7 and 11 show that, as expected, the precision of the velocity measurement mechanism dictates the maximum separation of reference points, if a limit on the expected error is imposed: if a good sonar/Doppler system is available, base-line arrays can be spread in a sparse way, while a noisy velocity measurement system imposes strict limits on the periods of autonomous navigation.